

Dynamics of beam pair coupled by visco-elastic interlayer

J. Náprstek^{a,*}, S. Hračov^a

^a*Institute of Theoretical and Applied Mechanics, ASCR v.v.i., Prosecká 76, 190 00 Praha, Czech Republic*

Received 3 November 2015; received in revised form 21 December 2015

Abstract

An exact method is presented for solving the vibration of a double-beam system subjected to harmonic excitation. The system consists of a loaded main beam and an auxiliary beam joined together using massless visco-elastic layer. The Euler-Bernoulli model is used for the transverse vibrations of beams, and the spring-dashpot represents a simplified model of viscoelastic material. The damping is assumed to be neither small nor proportional, and the forcing function can be either concentrated at any point or distributed continuously. The method involves a simple change of variables and modal analysis to decouple and to solve the governing differential equations respectively. A case study is solved in detail to demonstrate the methodology, and the frequency responses are shown in dimensionless parameters for low and high values of stiffness and damping of the interlayer. The analysis reveals two sets of eigen-modes: (i) the odd in-phase modes whose eigen-values and resonant peaks are independent of stiffness and damping, and (ii) the even out-of-phase modes whose eigen-values increase with raising stiffness and resonant peaks decrease with increasing damping. The closed-form solution and relevant plots (especially the three-dimensional ones) illustrate not only the principles of the vibration problem but also shed light on practical applications.

© 2015 University of West Bohemia. All rights reserved.

Keywords: double-beam dynamics, visco-elastic interlayer, kinematic damping

1. Introduction

Two parallel slender beams with a visco-elastic interlayer can serve as a relevant mathematical model of a number of engineering systems. The principle is analogous with the tuned mass damper (TMD) widely used to diminish vibration of high slender structures excited by strong dynamic effects of wind. A typical example is a double skin facade of tall buildings. The outer skin can be considered as a dynamic damper and thus contributes to comfort inside the building. Some information have been published rather in review papers having engineering character, see for instance [1, 2, 6] or books dealing with general wind engineering [3, 7].

A remarkable example of a realized structure which utilizes this principal of the damping is the “Tokyo Sky Tree”. It concerns the city transmission tower of the height 634 m, erected and opened in 2013, see Fig. 1. It consists of two coaxial parts coupled together by a large number of dashpots. Authors claim that possessing this equipment, the tower is able to weather an earthquake attack of 9.0 degree and adequate windstorm as well. Anyway detailed information are hardly accessible.

Many other applications emerge in power piping, when using two coaxial pipes with an interlayer in order to suppress vibration due to flow and structure interaction. Similar inconvenient behavior can exhibit panels which fall into the flutter post-critical state (panel flutter). Further applications can be expected at industrial chimneys, towers, etc. The idea of vibration damping

*Corresponding author. Tel.: +420 286 892 515, e-mail: naprstek@itam.cas.cz.

using such a formation is inspired by very well known TMD which is widely used in civil and mechanical engineering. Nevertheless its internal structure, function, limitations and singular states are incomparably more complicated. Therefore adequate applications should be cautious and possible recommendations addressed to designers of such devices should be thought out carefully.

In any case the system being based on two continuous beams with a visco-elastic interlayer looks to be very promising. It is suitable to work not only in one frequency domain like a conventional TMD, but can serve in several frequency domains and therefore it is appropriate to be used in a broad band excitation environment.

The paper presents a detailed analysis of eigen and forced vibration of the double-beam system with massless visco-elastic interlayer. Some partial cases have been already discussed in literature in the past, see for instance [4, 5, 8]. However mathematical aspects of this problem are still rather limited and should be treated at the level obvious in Rational Mechanics.



Fig. 1. “Tokyo Sky Tree” transmission tower

2. Basic considerations

Linear eigen and forced vibrations of two parallel beams with massless visco-elastic interlayer are investigated. Simple Euler-Bernoulli models with prismatic cross section are considered. Thickness of the interlayer is constant. Boundary conditions can be basically adopted in any arbitrary configuration, nevertheless certain frequently used settings are discussed in order to keep some analogy with real structures. Three possible schemes are obvious from Fig. 2. So that we can formulate the differential system:

$$\begin{aligned} EJ_1 u_1'''' + b_1 \dot{u}_1 + b(\dot{u}_1 - \dot{u}_2) + c(u_1 - u_2) + \mu_1 \ddot{u}_1 &= f(x, t), \\ EJ_2 u_2'''' + b_2 \dot{u}_2 + b(\dot{u}_2 - \dot{u}_1) + c(u_2 - u_1) + \mu_2 \ddot{u}_2 &= 0, \end{aligned} \quad (1)$$

where geometric and physical parameters of both beams and interlayer are considered constant independent on the length coordinate, see Fig. 2. In particular the following nomenclature has been adopted: EJ_i – bending stiffness of i -th beam ($i = 1, 2$) [Nm^2]; μ_i – mass/length of the adequate beam [Ns^2m^{-2}]; b_i , b – viscous damping/length of adequate beam or interlayer respectively [Nsm^{-2}]; c – normal stiffness of the interlayer/length [Nm^{-2}]; $f(x, t)$ – excitation force/length [Nm^{-1}]. There are a priori neglected (i) beams: shear deformability, cross-section rotation inertia, static length force (Euler-Bernoulli beams are considered); (ii) interlayer: shear stiffness, shear damping.

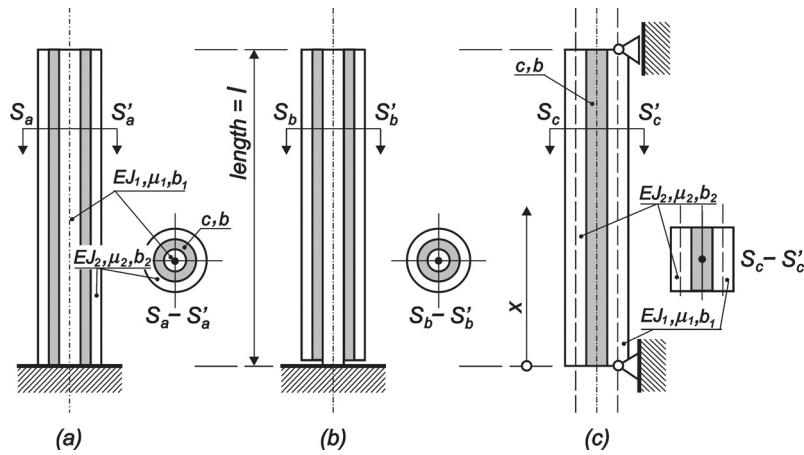


Fig. 2. Outline of structures with interlayer: (a) two coaxial cylindrical consoles, (b) two coaxial slender cylinders - inner is on one side fully clamped while outer one is free on both sides, (c) two parallel beams, beam (1) is simply supported, beam (2) is free on both sides

As stationary processes only will be investigated in the meaning of eigen vibration or forced vibration due to stationary excitation of $f(x, t) = F(x)e^{i\omega t}$ type, than space and time coordinates in functions $u_1 = u_1(x, t)$, $u_2 = u_2(x, t)$ can be separated and moreover the response time history in harmonic form with the frequency ω can be adopted. Hence displacements $u_1(x, t)$, $u_2(x, t)$ enable to be written in the form as commonly used:

$$u_1(x, t) = v_1(x) \cdot e^{i\omega t}, \quad u_2(x, t) = v_2(x) \cdot e^{i\omega t}. \tag{2}$$

Substituting expressions from (2) into the basic system given by (1) one obtains:

$$\begin{aligned} v_1''''(x) - (\lambda_1^4 - i\beta_1)v_1(x) - (\gamma_1 + i\delta_1)v_2(x) &= F(x)/EJ_1, \\ v_2''''(x) - (\gamma_2 + i\delta_2)v_1(x) - (\lambda_2^4 - i\beta_2)v_2(x) &= 0, \end{aligned} \tag{3}$$

where it has been denoted:

$$\begin{aligned} \lambda_1^4 &= \frac{\mu_1\omega^2 - c}{EJ_1}, & \beta_1 &= \frac{b_1 + b}{EJ_1} \omega, & \gamma_1 &= \frac{c}{EJ_1}, & \delta_1 &= \frac{b\omega}{EJ_1}, \\ \lambda_2^4 &= \frac{\mu_2\omega^2 - c}{EJ_2}, & \beta_2 &= \frac{b_2 + b}{EJ_2} \omega, & \gamma_2 &= \frac{c}{EJ_2}, & \delta_2 &= \frac{b\omega}{EJ_2}. \end{aligned} \tag{4}$$

A solution of the homogeneous differential system in (3) can be written in the form:

$$v_1(x) = V_1e^{\psi x}, \quad v_2(x) = V_2e^{\psi x} \quad \text{and} \quad v_1''''(x) = V_1\psi^4e^{\psi x}, \quad v_2''''(x) = V_2\psi^4e^{\psi x}, \tag{5}$$

which provides a homogeneous algebraic system:

$$\begin{bmatrix} \psi^4 - \Lambda_1^4 & -q_1 \\ -q_2 & \psi^4 - \Lambda_2^4 \end{bmatrix} \cdot \begin{bmatrix} V_1 \\ V_2 \end{bmatrix} = 0, \tag{6}$$

where

$$\Lambda_1^4 = \lambda_1^4 - i\beta_1, \quad q_1 = \gamma_1 + i\delta_1, \quad \Lambda_2^4 = \lambda_2^4 - i\beta_2, \quad q_2 = \gamma_2 + i\delta_2. \tag{7}$$

The determinant of the system, equation (6), should vanish:

$$(\psi^4 - \Lambda_1^4)(\psi^4 - \Lambda_2^4) - q_1q_2 = 0, \tag{8}$$

which means:

$$\begin{aligned} \Psi_1^4 = \psi_{1-4}^4 &= \frac{1}{2} [A + (A^2 + B^2)^{1/2}], & \Psi_2^4 = \psi_{5-8}^4 &= \frac{1}{2} [A - (A^2 + B^2)^{1/2}], \\ A = \Lambda_1^4 + \Lambda_2^4, & B^2 = -4\Lambda_1^4\Lambda_2^4 + 4q_1q_2, & D^2 = A^2 + B^2 &= (\Lambda_1^4 - \Lambda_2^4)^2 + 4q_1q_2. \end{aligned} \quad (9)$$

Let us proceed to the vector $[V_1, V_2]^T$, see (6). With respect to (8) and symbolics introduced in (9), one can determine $[V_1, V_2]^T$ up to the multiplication constant dissembling the matrix in (6) with respect to the first row inserting successively $\psi^4 = \Psi_1^4$ and Ψ_2^4 :

$$\begin{aligned} V_{11} = V_{1,1-4} &= \Psi_1^4 - \Lambda_2^4 = \frac{1}{2} [\Lambda_1^4 - \Lambda_2^4 + ((\Lambda_1^4 - \Lambda_2^4)^2 + 4q_1q_2)^{1/2}], & V_{21} = V_{2,1-4} &= q_2, \\ V_{12} = V_{1,5-8} &= \Psi_2^4 - \Lambda_2^4 = \frac{1}{2} [\Lambda_1^4 - \Lambda_2^4 - ((\Lambda_1^4 - \Lambda_2^4)^2 + 4q_1q_2)^{1/2}], & V_{22} = V_{2,5-8} &= q_2, \end{aligned} \quad (10)$$

where $[V_{11}, V_{21}]^T$ corresponds with Ψ_1^4 while $[V_{12}, V_{22}]^T$ with Ψ_2^4 . These roots satisfy (6) either due to zero determinant, equation (8), or directly.

3. Beams and interlayer without damping

3.1. General solution

Let us examine eigen-values and eigen-modes in case when the viscous damping of beams and interlayer vanishes, i.e. $b_1 = b_2 = b = 0$. Parameters $\Lambda_1^4, \Lambda_2^4, q_1, q_2$ following relations (4) become real and therefore ψ^4 is real either positive or negative. Distribution of the roots ψ_{1-4} and ψ_{5-8} around the unit circle is:

$$\alpha_{1-4}^4 = +1 \Rightarrow \alpha_{1-4} = \begin{pmatrix} \pm 1 \\ \pm i \end{pmatrix}, \quad \alpha_{5-8}^4 = -1 \Rightarrow \alpha_{5-8} = \frac{\pm 1 \pm i}{\sqrt{2}}. \quad (11)$$

Parameters A, B and ω_a^2, ω_b^2 have the form:

$$\begin{aligned} A^2 &= \left(\frac{\mu_1\omega^2 - c}{EJ_1} + \frac{\mu_2\omega^2 - c}{EJ_2} \right)^2, & B^2 &= \frac{-\mu_1\mu_2\omega^4 + c\omega^2(\mu_1 + \mu_2)}{EJ_1EJ_2}, \\ \omega_a^2 &= c \frac{EJ_1 + EJ_2}{EJ_1\mu_2 + EJ_2\mu_1}, & \omega_b^2 &= c \frac{\mu_1 + \mu_2}{\mu_1\mu_2}, \quad \text{it holds: } \omega_b^2 > \omega_a^2. \end{aligned} \quad (12)$$

See Fig. 3 for relation of A, B parameters as functions ω . Character of integral of homogeneous system (1) is specified by attributes of A, B . Therefore following intervals or special values of ω should be separately treated:

(a) $\omega^2 = 0, A < 0, B^2 = 0, \psi_{1-4}^4 = 0, \psi_{5-8}^4 < 0,$

$$\psi_{1-4} = 0, \quad \psi_{5-8} = (\pm 1 \pm i)\rho_2, \quad \rho_2 = \frac{1}{\sqrt{2}} \left(\frac{c}{EJ_1} + \frac{c}{EJ_2} \right)^{1/4}, \quad (13)$$

(b) $0 < \omega^2 < \omega_b^2, A < D, \psi_{1-4}^4 > 0, \psi_{5-8} < 0,$

$$\begin{aligned} \psi_{1-4} &= \begin{pmatrix} \pm 1 \\ \pm i \end{pmatrix} \cdot \rho_3, & \rho_3 &= (\frac{1}{2}A + \frac{1}{2}D)^{1/4}, \\ \psi_{5-8} &= (\pm 1 \pm i) \cdot \rho_4, & \rho_4 &= \frac{1}{\sqrt{2}}(\frac{1}{2}D - \frac{1}{2}A)^{1/4}, \\ \omega^2 < \omega_a^2 &\Rightarrow \rho_3 < \rho_4, & \omega_a^2 < \omega^2 < \omega_b^2 &\Rightarrow \rho_3 > \rho_4, \end{aligned} \quad (14)$$

note: $\omega^2 = \omega_a^2$ does not mean any turning point in solution types, only a quantitative difference,

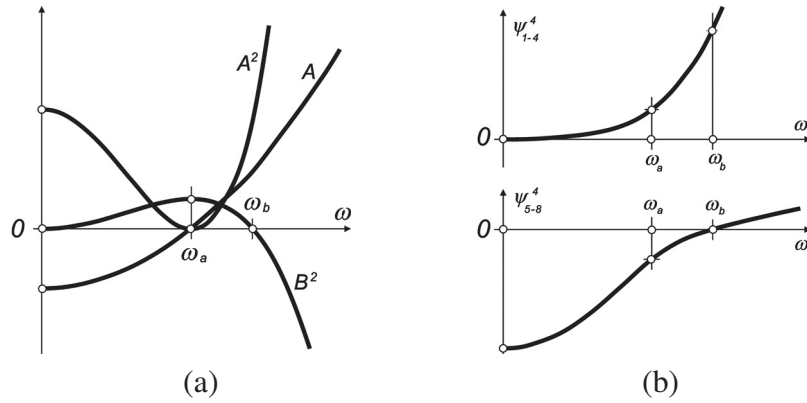


Fig. 3. Parameters and arguments as functions of the frequency ω : (a) Parameters A, A^2, B^2 , (b) Arguments $\psi_{1-4}^4, \psi_{5-8}^4$

(c) $\omega^2 = \omega_b^2, B = 0, A = D, \psi_{1-4}^4 > 0, \psi_{5-8}^4 = 0,$

$$\psi_{1-4} = \left\langle \begin{matrix} \pm 1 \\ \pm i \end{matrix} \right\rangle \cdot \rho_5, \rho_5 = A^{1/4} = (\lambda_1^4 + \lambda_2^4)^{1/4}, \quad \psi_{5-8} = 0, \quad (15)$$

(d) $\omega^2 > \omega_b^2, A > D, \psi_{1-4}^4 > 0, \psi_{5-8}^4 > 0,$

$$\begin{aligned} \psi_{1-4} &= \left\langle \begin{matrix} \pm 1 \\ \pm i \end{matrix} \right\rangle \cdot \rho_7, & \rho_7 &= \left(\frac{1}{2}A + \frac{1}{2}D\right)^{1/4}, \\ \psi_{5-8} &= \left\langle \begin{matrix} \pm 1 \\ \pm i \end{matrix} \right\rangle \cdot \rho_8, & \rho_8 &= \left(\frac{1}{2}A - \frac{1}{2}D\right)^{1/4}, \end{aligned} \quad \rho_7 > \rho_8. \quad (16)$$

Let us outline position of roots in the Gaussian complex plane, see Fig. 4, when ω^2 is increasing from zero throughout all partial intervals until a certain $\omega^2 > \omega_b^2$. The basic character of roots follows from (11). Roots ψ_{1-4}^4 and ψ_{5-8}^4 are moving from the left to the right on the real axis. We start with $\omega^2 = 0$ providing zero $\psi_{1-4}^4 = 0$ and negative $\psi_{5-8}^4 < 0$, see Fig. 4a, then passing interval $0 < \omega^2 < \omega_b^2$ one obtains $\psi_{1-4}^4 > 0$ and $\psi_{5-8}^4 < 0$ so that roots ψ_{1-4} are distributed on coordinate axes in a distance ρ_3 from the origin and similarly ψ_{5-8} on diagonals of quadrants with radius ρ_4 , see Fig. 4b. It follows a transition case $\omega^2 = \omega_b^2$ giving $\psi_{1-4}^4 > 0$ and $\psi_{5-8}^4 = 0$ which means that ψ_{1-4} lie at coordinate axes on a circle of diameter ρ_5 , see Fig. 4c. Finally whatever $\omega^2 > \omega_b^2$ leads to positive $\psi_{1-4}^4 > 0$ as well as $\psi_{5-8}^4 > 0$ and therefore provides always twice four roots only on coordinate axes distributed on concentric circles of diameters ρ_7, ρ_8 , see Fig. 4d.

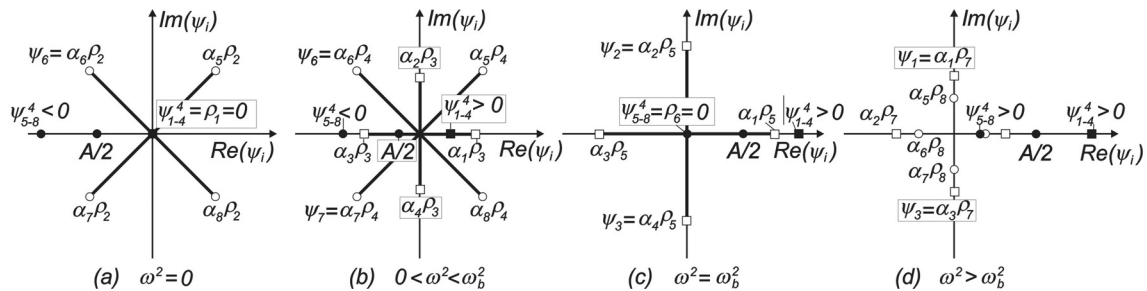


Fig. 4. Position of roots ψ_{1-4} and ψ_{5-8} in Gaussian complex plane in individual intervals ω^2 following (13)–(16) — damping is neglected

Avoiding any damping the vectors $[V_{1i}, V_{2i}]^T$, $i = 1, 2$, equations (10), can be written as follows:

$$\begin{aligned} V_{11} &= \frac{1}{2} [\lambda_1^4 - \lambda_2^4 + ((\lambda_1^4 - \lambda_2^4)^2 + 4\gamma_1\gamma_2)^{1/2}], & V_{21} &= \gamma_2, \\ V_{12} &= \frac{1}{2} [\lambda_1^4 - \lambda_2^4 - ((\lambda_1^4 - \lambda_2^4)^2 + 4\gamma_1\gamma_2)^{1/2}], & V_{22} &= \gamma_2. \end{aligned} \quad (17)$$

General solutions inherent to (5) in individual values and intervals of ω corresponding with (13), (14), (15), (16), can be formulated using Euler formulae:

(a) $\omega^2 = 0$:

$$\begin{aligned} \begin{vmatrix} v_1(x) \\ v_2(x) \end{vmatrix} &= \begin{vmatrix} V_{11} \\ V_{21} \end{vmatrix} \cdot (C_1 + C_2x + C_3x^2 + C_4x^3) + \\ &\begin{vmatrix} V_{12} \\ V_{22} \end{vmatrix} \cdot (C_5 \cosh \rho_2x \cdot \cos \rho_2x + C_6 \cosh \rho_2x \cdot \sin \rho_2x + \\ &C_7 \sinh \rho_2x \cdot \cos \rho_2x + C_8 \sinh \rho_2x \cdot \sin \rho_2x), \end{aligned} \quad (18)$$

(b) $0 < \omega^2 < \omega_b^2$:

$$\begin{aligned} rcl \begin{vmatrix} v_1(x) \\ v_2(x) \end{vmatrix} &= \begin{vmatrix} V_{11} \\ V_{21} \end{vmatrix} \cdot (C_1 \cos \rho_3x + C_2 \sin \rho_3x + C_3 \cosh \rho_3x + C_4 \sinh \rho_3x) + \\ &\begin{vmatrix} V_{12} \\ V_{22} \end{vmatrix} \cdot (C_5 \cosh \rho_4x \cdot \cos \rho_4x + C_6 \cosh \rho_4x \cdot \sin \rho_4x + \\ &C_7 \sinh \rho_4x \cdot \cos \rho_4x + C_8 \sinh \rho_4x \cdot \sin \rho_4x), \end{aligned} \quad (19)$$

(c) $\omega^2 = \omega_b^2$:

$$\begin{aligned} \begin{vmatrix} v_1(x) \\ v_2(x) \end{vmatrix} &= \begin{vmatrix} V_{11} \\ V_{21} \end{vmatrix} \cdot (C_1 \cos \rho_5x + C_2 \sin \rho_5x + C_3 \cosh \rho_5x + C_4 \sinh \rho_5x) + \\ &\begin{vmatrix} V_{12} \\ V_{22} \end{vmatrix} \cdot (C_5 + C_6 x + C_7 x^2 + C_8 x^3), \end{aligned} \quad (20)$$

(d) $\omega^2 > \omega_b^2$:

$$\begin{aligned} \begin{vmatrix} v_1(x) \\ v_2(x) \end{vmatrix} &= \begin{vmatrix} V_{11} \\ V_{21} \end{vmatrix} \cdot (C_1 \cos \rho_7x + C_2 \sin \rho_7x + C_3 \cosh \rho_7x + C_4 \sinh \rho_7x) + \\ &\begin{vmatrix} V_{12} \\ V_{22} \end{vmatrix} \cdot (C_5 \cos \rho_8x + C_6 \sin \rho_8x + C_7 \cosh \rho_8x + C_8 \sinh \rho_8x). \end{aligned} \quad (21)$$

The particular solution, equation (19), should continuously pass into (18) for $\omega \rightarrow 0$ and into (20) for $\omega \rightarrow \omega_b$ from below. Similarly the particular solution (21) when $\omega \rightarrow \omega_b$ from above. Limitations of (19) or (21) to $\omega = 0$ or $\omega = \omega_b$ should be done via relevant decompositions around $\omega = 0$ or $\omega = \omega_b$ in order to pass smoothly into (18) or (20).

Let us introduce boundary conditions corresponding to Fig. 2a. Both beams are consoles and eigen-value problem is considered, which means:

$$\begin{aligned} v_1(0) = 0, & \quad v_1'(0) = 0, & \quad v_1''(l) = 0, & \quad v_1'''(l) = 0, \\ v_2(0) = 0, & \quad v_2'(0) = 0, & \quad v_2''(l) = 0, & \quad v_2'''(l) = 0. \end{aligned} \quad (22)$$

The problem will be discussed at the interval $\omega^2 > \omega_b^2$. Regarding the general solution of the type (d), equations (21), one can carry out a system of eight algebraic equations for unknown integration constants $C_1 - C_8$:

$$\begin{aligned}
 \begin{pmatrix} v_1(0) \\ v_1'(0) \\ v_2(0) \\ v_2'(0) \\ v_1''(l) \\ v_1'''(l) \\ v_2''(l) \\ v_2'''(l) \end{pmatrix} &= \begin{pmatrix} V_{11}, & 0, & V_{11}, & 0, \\ 0, & V_{11}\rho_7, & 0, & V_{11}\rho_7, \\ V_{21}, & 0, & V_{21}, & 0, \\ 0, & V_{21}\rho_7, & 0, & V_{21}\rho_7, \\ -V_{11}\rho_7^2 C_{s7}, & -V_{11}\rho_7^2 S_{n7}, & V_{11}\rho_7^2 C_{h7}, & V_{11}\rho_7^2 S_{h7}, \\ V_{11}\rho_7^3 S_{n7}, & -V_{11}\rho_7^3 C_{s7}, & V_{11}\rho_7^3 S_{h7}, & V_{11}\rho_7^3 C_{h7}, \\ -V_{21}\rho_7^2 C_{s7}, & -V_{21}\rho_7^2 S_{n7}, & V_{21}\rho_7^2 C_{h7}, & V_{21}\rho_7^2 S_{h7}, \\ V_{21}\rho_7^3 S_{n7}, & -V_{21}\rho_7^3 C_{s7}, & V_{21}\rho_7^3 S_{h7}, & V_{21}\rho_7^3 C_{h7}, \end{pmatrix} \\
 & \cdot \begin{pmatrix} V_{12}, & 0, & V_{12}, & 0 \\ 0, & V_{12}\rho_8, & 0, & V_{12}\rho_8 \\ V_{22}, & 0, & V_{22}, & 0 \\ 0, & V_{22}\rho_8, & 0, & V_{22}\rho_8 \\ -V_{12}\rho_8^2 C_{s8}, & -V_{12}\rho_8^2 S_{n8}, & V_{12}\rho_8^2 C_{h8}, & V_{12}\rho_8^2 S_{h8} \\ V_{12}\rho_8^3 S_{n8}, & -V_{12}\rho_8^3 C_{s8}, & V_{12}\rho_8^3 S_{h8}, & V_{12}\rho_8^3 C_{h8} \\ -V_{22}\rho_8^2 C_{s8}, & -V_{22}\rho_8^2 S_{n8}, & V_{22}\rho_8^2 C_{h8}, & V_{22}\rho_8^2 S_{h8} \\ V_{22}\rho_8^3 S_{n8}, & -V_{22}\rho_8^3 C_{s8}, & V_{22}\rho_8^3 S_{h8}, & V_{22}\rho_8^3 C_{h8} \end{pmatrix} \cdot \begin{pmatrix} C_1 \\ C_2 \\ C_3 \\ C_4 \\ C_5 \\ C_6 \\ C_7 \\ C_8 \end{pmatrix} = \begin{pmatrix} 0 \\ 0 \\ 0 \\ 0 \\ 0 \\ 0 \\ 0 \\ 0 \end{pmatrix}, \tag{23}
 \end{aligned}$$

where following notation has been used:

$$\begin{aligned}
 C_{s7} = \cos \rho_7 l, \quad S_{n7} = \sin \rho_7 l, \quad C_{h7} = \cosh \rho_7 l, \quad S_{h7} = \sinh \rho_7 l, \\
 C_{s8} = \cos \rho_8 l, \quad S_{n8} = \sin \rho_8 l, \quad C_{h8} = \cosh \rho_8 l, \quad S_{h8} = \sinh \rho_8 l. \tag{24}
 \end{aligned}$$

For modal properties eigen-values and eigen-vectors of the square matrix in (23) are to be found out. If the response due to harmonic excitation with the frequency ω at boundaries is investigated, the system (23) for relevant non-homogeneous right side should be solved and integration constant substitute backwards into (21).

3.2. Special configuration of structural parameters of beams

Special case of structural parameters has been considered regarding following relation of parameters:

$$EJ_2/EJ_1 = k_{EJ} = k_\mu = \mu_2/\mu_1, \quad \text{or} \quad \mu_1/EJ_1 = \mu_2/EJ_2. \tag{25}$$

Fulfilment of this relation provides the identical modal properties of both individual beams. The typical solution of the determinant of the square matrix in (23) related to this system is depicted as a function of ω in Fig. 5. In all numerical simulations the following structural parameters of the beams have been used: $EJ_1 = 8.1 \text{ GNm}^2$, $\mu_1 = 660.5 \text{ N s}^2\text{m}^{-2}$, $l = 100 \text{ m}$, $k_{EJ} = k_\mu = 1/3$.

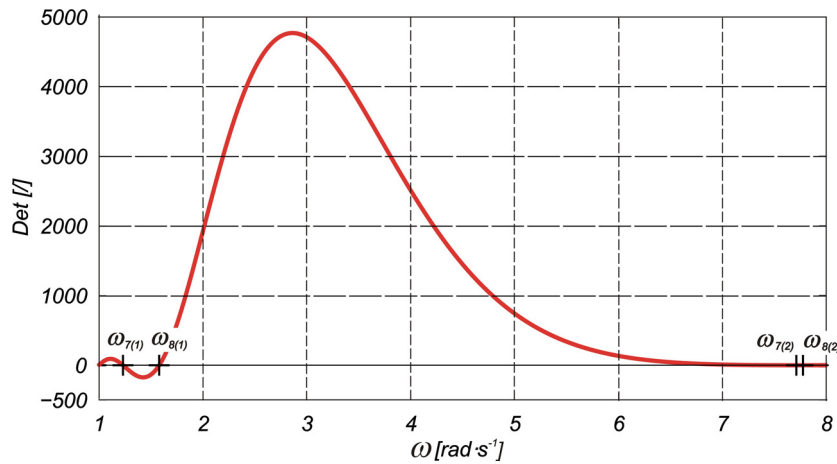


Fig. 5. Determinant of the system as a function of ω ($c = 162 \text{ Nm}^{-2}$)

The zero values of the determinant, i.e. eigen-values of the system, are equal to the roots of characteristic equation, which splits into two equations:

$$1 + \cos \rho_7 l \cdot \cosh \rho_7 l = 0, \quad 1 + \cos \rho_8 l \cdot \cosh \rho_8 l = 0, \quad (26)$$

providing two groups of the roots (even and odd). Take a note that each of (26) represents a characteristic equation typical for a cantilever beam.

The odd eigen-values and eigen-modes are related to ρ_7 :

$$\rho_7^A = \frac{\mu_1 \omega^2}{E J_1} = \frac{\mu_2 \omega^2}{E J_2} \Rightarrow \omega_{7(j)}, \quad j = 1, 2, \dots, \quad (27)$$

where subscript $7(j)$ in $\omega_{7(j)}$ means adjointness with the ρ_7 root and j is a number of the couple of eigen-values (see also symbolics used in Fig. 5). The above eigen-values are independent from the interlayer stiffness and identical with those of the individual beams. The equality between elements of vector V :

$$V_{11} = V_{21}, \quad (28)$$

leads to the same amplitude as well as the phase of the corresponding points on both beams during the free vibration associated with odd modes, see Fig. 6.

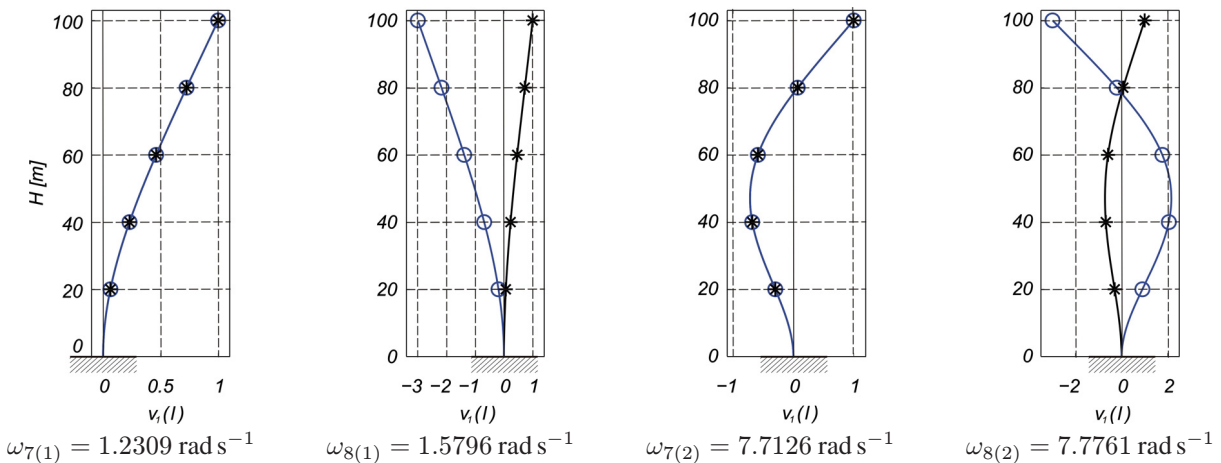


Fig. 6. The first four eigen-modes of the beam pair coupled by visco-elastic interlayer (black line – primary beam, blue line – secondary beam, $c = 162 \text{ Nm}^{-2}$)

The even eigen-values related to:

$$\rho_8^4 = \frac{\mu_1 \omega^2}{EJ_1} - c \frac{EJ_1 + EJ_2}{EJ_1 \cdot EJ_2} \Rightarrow \omega_{8(j)}, \quad j = 1, 2, \dots \quad (29)$$

are equal to the eigen-values of the system represented by individual cantilever beam supported by an elastic layer. The effective stiffness of this fictive layer is a function of the interlayer stiffness and of the beams stiffnesses ratio. Similarly like before the subscript $8(j)$ means adjointness with ρ_8 root and j is a number of the couple of eigen-values. Even eigen-modes are also composed from the modes of individual beams. In contrary to the odd modes, the phase between corresponding points on both beams is opposite. The ratio of the amplitudes of the points is constant and equal to a ratio of the stiffness of the beams:

$$V_{12} = -k_{EJ} V_{22}. \quad (30)$$

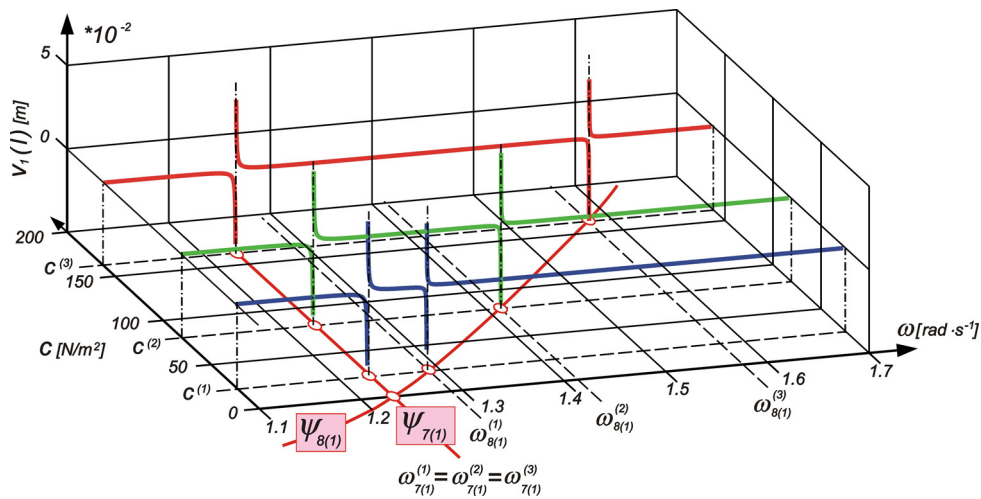


Fig. 7. Top deflection of the primary beam as a function of ω for several stiffness c

The influence of the stiffness c on the eigen-values of the system is shown in Fig. 7. The deflection at the top of the primary beam excited by the harmonic force is depicted as a function of ω . The first asymptote, which indicates the position of the first eigen-value, is obviously common for every c being independent from this one. It is related with the root $\psi_{7(j)}$ leading to eigen-values $\omega_{7(j)}^{(k)}$, where $j = 1, 2$ is a number of eigen-values couple and $k = 1, 2, 3$ means number of interlayer stiffness considered $c^{(1)}, c^{(2)}, c^{(3)}$, see Fig. 7; compare with red highlighted boxes in Fig. 8. The eigen-values of the even group are increasing with the raising c . It corresponds with the root $\psi_{8(j)}$ providing eigen-values $\omega_{8(j)}^{(k)}$ with analogous symbolics used in sub- and super-scripts.

It is worthy to get an overview about an influence of the interlayer stiffness c onto the distribution of eigen-values in the plane (ω, c) . Such a picture will complete appropriately Fig. 7 of top deflection resonance curves.

Let us recall formulae (27) and (29) for ρ_7^4, ρ_8^4 and (12) for ω_b^2 . Considering (26), several first roots (odd and even) have been evaluated:

$$\rho_{7(1)} = \rho_{8(1)} = 1.8751/l, \quad \rho_{7(2)} = \rho_{8(2)} = 4.6941/l, \quad \rho_{7(3)} = \rho_{8(3)} = 7.8543/l, \quad \dots \quad (31)$$

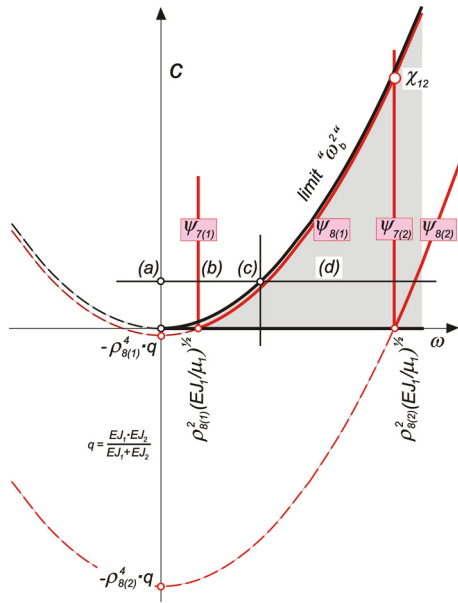


Fig. 8. Distribution of eigen-values in the plane (ω, c)

Couples of eigen-values as functions of ω can be plotted in the plane (ω, c) :

$$\frac{\mu_1 \omega^2}{EJ_1} = \rho_{7(j)}^4, \quad c = \left(\frac{\mu_1 \omega^2}{EJ_1} - \rho_{8(j)}^4 \right) \frac{EJ_1 \cdot EJ_2}{EJ_1 + EJ_2}. \quad (32)$$

There are plotted in Fig. 8 two couples for $j = 1, 2$. We can see that parabolas representing the even roots are identical for every j . They differ only by position of the apex on the c axis. The figure shows that every even root can cross the vertical line of every odd roots of the level $k > j$ on the value $c > 0$:

$$c = (\rho_{8(k)}^4 - \rho_{8(j)}^4) \cdot \frac{EJ_1 \cdot EJ_2}{EJ_1 + EJ_2}, \quad (33)$$

see e.g. the point χ_{12} . At this point a double eigen-value exists corresponding simultaneously to the even eigen-mode of the first couple and the odd eigen-mode of the second couple, see Fig. 8.

Difference rate of even and odd roots in every couple when increasing c can be estimated at the ω axis by the first derivative of the second part of (32):

$$\Delta_j = 2 \sqrt{\frac{\mu_1}{EJ_1}} \cdot \rho_{8(j)}^2. \quad (34)$$

Therefore the difference rate of even and odd roots at the ω axis is decreasing with raising j as it could be seen also in Fig. 5.

It is useful to determine the limit of results validity which have been carried out for the case $\omega^2 > \omega_b^2$. It follows immediately from (12):

$$c = \omega^2 \frac{\mu_1 \cdot \mu_2}{\mu_1 + \mu_2}. \quad (35)$$

Taking into account constraints (25) it can be easily shown that openings of the parabola (35) and that following from the second part of (32) are identical. The parabola (35) passes the origin and therefore it cannot intersect them. This parabola delimits validity of results (13)–(16) and (18)–(21) obtained for non-damped system, see Fig. 8. Using this picture, it can be decided, which roots evaluated using (26) are valid and which should be rejected.

4. Beams and interlayer with damping

4.1. General solution — damped interlayer

Investigating a real structure it can be supposed that the damping of beams is small in comparison with that of the interlayer. Therefore recalling (6)–(9) we can adopt $b_1 = b_2 = 0$ and $b > 0$, which means that $\beta_1 = \delta_1 > 0$ and $\beta_2 = \delta_2 > 0$. Thus $\Lambda_1^4, \Lambda_2^4, q_1, q_2$ are complex similarly like A, B^2, D^2 and roots $\Psi_1, \Psi_2, \psi_{1-4}, \psi_{5-8}$. Consequently, we can write:

$$\begin{aligned} A &= A_r + iA_i = \lambda_1^4 + \lambda_2^4 - i(\delta_1 + \delta_2), \\ A^2 &= A_{r2} + iA_{i2} = (\lambda_1^4 + \lambda_2^4)^2 - (\delta_1 + \delta_2)^2 - 2i(\lambda_1^4 + \lambda_2^4)(\delta_1 + \delta_2), \\ B^2 &= B_{r2} + iB_{i2} = -4(\lambda_1^4 \lambda_2^4 - \gamma_1 \gamma_2) + 4i((\lambda_1^4 + \gamma_1)\delta_2 + (\lambda_2^4 + \gamma_2)\delta_1), \\ D^2 &= D_{r2} + iD_{i2} = (\lambda_1^4 - \lambda_2^4)^2 + 4\gamma_1 \gamma_2 - (\delta_1 + \delta_2)^2 - \\ &\quad 2i((\lambda_1^4 - \lambda_2^4 - 2\gamma_2)\delta_1 - (\lambda_1^4 - \lambda_2^4 + 2\gamma_1)\delta_2), \\ D &= D_r + iD_i, \quad D_r^2 = \frac{1}{2} \left(D_{r2} + \sqrt{D_{r2}^2 + D_{i2}^2} \right), \quad D_i^2 = \frac{1}{2} \left(-D_{r2} + \sqrt{D_{r2}^2 + D_{i2}^2} \right). \end{aligned} \tag{36}$$

With respect to (9) it can be written:

$$\psi_{1-4}^4 = \frac{1}{2}(A_r + D_r + i(A_i + D_i)), \quad \psi_{5-8}^4 = \frac{1}{2}(A_r - D_r + i(A_i - D_i)), \tag{37}$$

which leads to individual roots:

$$\begin{aligned} j = 1-4 : \quad \psi_j &= \rho_{c1} \exp \left(\frac{i}{4}(\varphi_{c1} + (j-1)\pi) \right), \\ \rho_{c1} &= \left(\frac{1}{4}(A_r + D_r)^2 + \frac{1}{4}(A_i - D_i)^2 \right)^{1/8}, \quad \varphi_{c1} = \arctg \frac{A_i + D_i}{A_r + D_r}, \\ j = 5-8 : \quad \psi_j &= \rho_{c2} \exp \left(\frac{i}{4}(\varphi_{c2} + (j-1)\pi) \right), \\ \rho_{c2} &= \left(\frac{1}{4}(A_r - D_r)^2 + \frac{1}{4}(A_i - D_i)^2 \right)^{1/8}, \quad \varphi_{c2} = \arctg \frac{A_i - D_i}{A_r - D_r}, \\ \exp \left(\frac{i}{4}(j-1)\pi \right) &= \begin{pmatrix} \pm 1 \\ \pm i \end{pmatrix}, \quad \exp \left(\frac{i}{4}\varphi_{ck} \right) = \cos \frac{1}{4}\varphi_{ck} + i \sin \frac{1}{4}\varphi_{ck}, \quad k = 1, 2. \end{aligned} \tag{38}$$

Position of roots in the Gaussian plain can be transparently demonstrated enhancing configurations described for non damped case presented in Fig. 4. Fig. 9a demonstrates an event $\omega = 0$

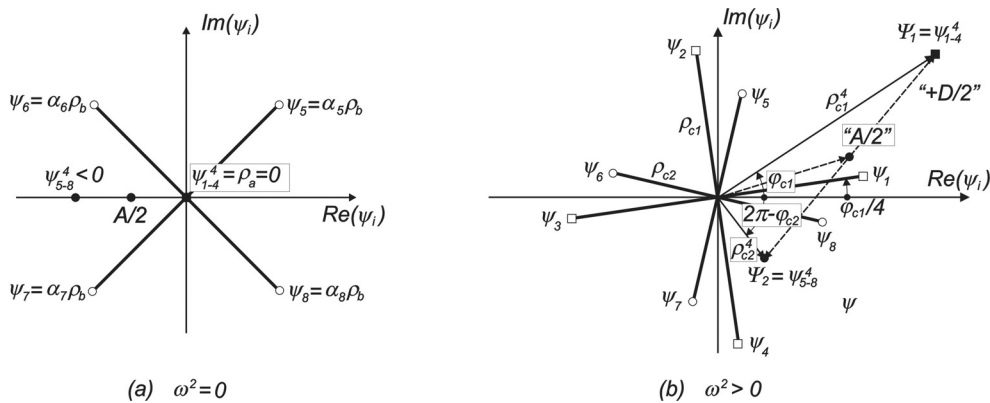


Fig. 9. Position of roots ψ_{1-4} and ψ_{5-8} in Gaussian complex plane for damped system; (a) $\omega^2 = 0$; (b) $\omega^2 > 0$

which is certainly identical with that for non damped configuration. Concerning Fig. 9b, it encompasses in a certain meaning paragraphs (b)–(d) discussed in subsection 3.1. Position of $\Psi_1 = \psi_{1-4}^4$ and $\Psi_2 = \psi_{5-8}^4$ in Gaussian plane is obviously given by vector summation of “ $A/2$ ” and “ $\pm D/2$ ” or being depicted in the picture by absolute values ρ_{c1}, ρ_{c2} and arguments $\varphi_{c1}, \varphi_{c2}$. The fourth roots of both Ψ_1, Ψ_2 provides distinct rosettes $\psi_1 - \psi_4$ and $\psi_5 - \psi_8$.

Moving in Gaussian plane, we cannot reach the origin (the special case $\omega^2 = \omega_b^2$ — par. (c)). To end up into this point would require $B_{r2} = B_{i2} = 0$ which is not possible with respect to (36) as far as $\omega > 0$.

As regards comparison with paragraphs (b) and (d), they enable to be processed together when consistently all parameters are understood as complex values. Therefore the general solution for every $\omega > 0$ can be formulated simply as follows:

$$\begin{aligned} \begin{vmatrix} v_1(x) \\ v_2(x) \end{vmatrix} &= \begin{vmatrix} V_{11} \\ V_{21} \end{vmatrix} \cdot (C_1 \cos \psi_1 x + C_2 \sin \psi_1 x + C_3 \cosh \psi_1 x + C_4 \sinh \psi_1 x) + \\ &\begin{vmatrix} V_{12} \\ V_{22} \end{vmatrix} \cdot (C_5 \cos \psi_5 x + C_6 \sin \psi_5 x + C_7 \cosh \psi_5 x + C_8 \sinh \psi_5 x), \end{aligned} \quad (39)$$

where ψ_1, ψ_5 are complex numbers given by (38) ($j = 1, 5$). Considering Euler’s formula they read:

$$\psi_1 = \rho_{c1} \left(\cos \frac{1}{4} \varphi_{c1} + i \sin \frac{1}{4} \varphi_{c1} \right), \quad \psi_5 = \rho_{c2} \left(\cos \frac{1}{4} \varphi_{c2} + i \sin \frac{1}{4} \varphi_{c2} \right). \quad (40)$$

Parameters $V_{11} - V_{22}$ have the original form corresponding to (10). Integration constants $C_1 - C_8$ are complex numbers. Taking into account that the solution (39) is formally of the same shape as the solution (21), equation (23) remains in force if there are replaced: $\rho_7 \rightarrow \psi_1, \rho_8 \rightarrow \psi_5$. The new algebraic system includes 16 real unknowns representing real and imaginary parts of $C_1 - C_8$. Components of the forced vibration can be evaluated and subsequently also absolute values of displacements or forces. It should be noted that the relevant determinant never reaches zero, unless ω is admitted also to be complex. In such a case true eigen-values in Gaussian plane can be evaluated as $\omega_j = \omega_{rj} + i\omega_{ij}$. Hence amplitudes of forced vibration exhibit on the real axis ω a certain maximum indicating only that in the proximity exists an adjoint eigen-value of the non damped system.

4.2. Special configuration of structural parameters of beams and damped interlayer

Analytical considerations of the previous subsection 4.1 are evaluated numerically in order to become aware of a quantitative influence of the interlayer viscous damping. The excitation is due to the unit shear force at the top of the primary beam. Three interlayer stiffnesses have been chosen $c^{(j)} = 24, 81, 162 \text{ Nm}^{-2}$ ($j = 1-3$). Every stiffness has been evaluated for four values of the damping: $b = 0, 1, 2, 7 \text{ Nsm}^{-2}$. Results are plotted in Fig. 10a–f. Pictures (a), (b) concern the stiffness $c^{(1)} = 24 \text{ Nm}^{-2}$, in particular picture (a) represents absolute value of the top deflection $|v_1(l)|$ while picture (b) regards the phase shift $f(l)$ in the same point. Curves plotted in various colors demonstrate results for individual values of the damping b . Similarly are organized also pictures (c), (d) and (e), (f), respectively. Interval $\omega = (0, 2.0)$ has been examined and therefore the system behavior in area of the first odd and even eigen-values has been demonstrated.

It is apparent that the position of the first odd eigen-value remained untouched, as the damping element did not in fact involve. Hence also the phase shift reveals a sudden jump of 180° in the point $\omega_{7(1)} = 1.2309 \text{ rad s}^{-1}$ independently from the interlayer stiffness. The neighborhood of the first even eigen-value $\omega_{8(1)} = 1.5796 \text{ rad s}^{-1}$ ($c = 162 \text{ Nm}^{-2}$) has a character as commonly

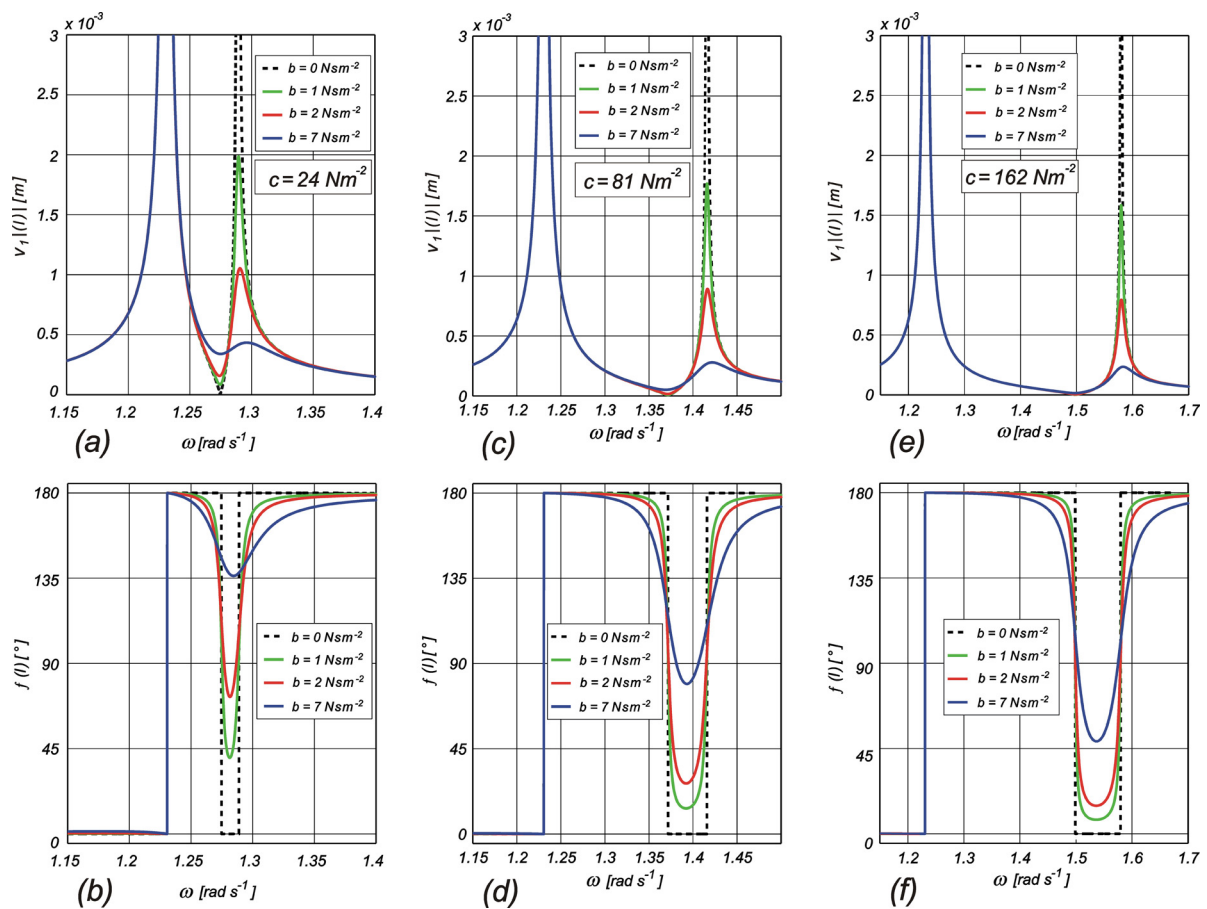


Fig. 10. Absolute value of the top deflection $|v_1(l)|$ and phase shift $f(l)$ for various interlayer stiffness c and damping ratio b : (a)–(b) $c = 24 \text{ Nm}^{-2}$, (c)–(d) $c = 81 \text{ Nm}^{-2}$, (e)–(f) $c = 162 \text{ Nm}^{-2}$

known at 2DOF system with a viscous damping. Between both eigen-values lies zero or a minimum of the system response $|v_1(l)|$. Similarly like on a 2DOF discrete system also here the response passes zero only if the damping vanishes, otherwise only a certain positive wave is exhibited which is getting to disappear with increasing damping level. Hence here is a domain of optimization of the vibration damping effect. Take a note, that the careful tuning is necessary, as this mechanism is exactly valid for distinctly expressed deterministic excitation frequency, while in practice we encounter the broad band excitation (mostly of the random type).

It is obvious that the damping effect is slightly increasing with raising stiffness of the interlayer, however also this fact should be handled with caution. Take a note that the system behaves similarly also in area of higher couples of eigen-values, although the sensitivity to parameters and tuning is higher.

5. Conclusion

The pair of beams with continuously distributed stiffness, mass and other parameters connected together by visco-elastic layer can be considered as a mechanism suitable to be used for suppression of structural vibration similarly like the tuned mass damper. The strength of the system with continuously distributed parameters consists in the fact that it can act in a wide frequency domain due to advantageous distribution of eigen-values on the frequency axis.

Detailed analysis has been performed for the special configuration of parameters and boundary conditions. In particular both beams have a character of a console and identical ratio of bending stiffness and mass. This composition makes possible to separate distinctly eigen-values into two groups: (i) odd – independent on the interlayer stiffness and (ii) even – being significantly influenced by this one. Each one of the latter group is able to work approximately as an independent vibration absorber. This scheme enabled to carry out a comprehensive analysis of interaction of system parts in a wide frequency domain.

Numerical evaluation of analytical results as presented in this paper has been step by step verified with those obtained by means of independent FEM analysis. Coincidence was perfect and thus challenging to continue this research.

Let us take a note that other combinations of boundary conditions and parameters being outside settings discussed here do not enable the full separation of dynamic parameters like those investigated in the paper. The aim of the paper was essentially to show qualitative character of system consisting of two beams with visco-elastic interlayer. General combinations of parameters require to deal with full 4th order characteristic equation. Therefore perturbation strategies should be used separating the original system into several disjoint groups which should be analysed independently. The same holds regarding general combination of boundary conditions. On the other hand it reveals that differences are only quantitative although more steps are necessary to be performed on numerical basis and consequently a careful assessment of approximate solutions applicability is to be done. Nevertheless the system keeps the basic character of dynamic properties. Analytical results obtained are in force and remain applicable to tune and optimize the damping effect.

Acknowledgements

The kind support of the Czech Science Foundation projects No. 13-41574P, 15-01035S and of the RVO 68378297 institutional support are gratefully acknowledged.

Reference

- [1] Fu, T. S., Double skin facades as mass dampers, Proceedings of American Control Conference, Washington DC, 2013, pp. 4 749–4 753.
- [2] Kareem, A., Kijewski, T., Tamura, Y., Mitigation of motions of tall buildings with specific examples of recent applications, *Wind and Structures* 2 (3) (1999) 201–251.
- [3] Koloušek, V., Pirner, M., Fischer, O., Náprstek, J., *Wind effects on civil engineering structures*, Elsevier, Amsterdam, 1984.
- [4] Kukla, S., Free vibration of the system of two beams connected by many translational springs, *Journal Sound and Vibration* 172 (1) (1994) 130–135.
- [5] Kyoung, S. M., Structural design of double skin facades as damping devices for tall buildings, *Procedia Engineering* 14 (2011) 1 351–1 358.
- [6] Passoni, C., Belleri, A., Marini, A., Riva, P., Existing structures connected with dampers: state of the art and future developments, Proceedings of the 2nd European Conference on Earthquake Engineering and Seismology, Istanbul, EAEE, 2014, 12 pgs.
- [7] Simiu, E., Scanlan, R. H., *Wind effects on structures: Fundamentals and applications to design*, 3rd Edition, Wiley, New York, 1996.
- [8] Vu, H. V., Ordoñez, A. M., Karnopp, B. H., Vibration of a double-beam system, *Journal Sound and Vibration* 229 (4) (2000) 807–822.